

Communication

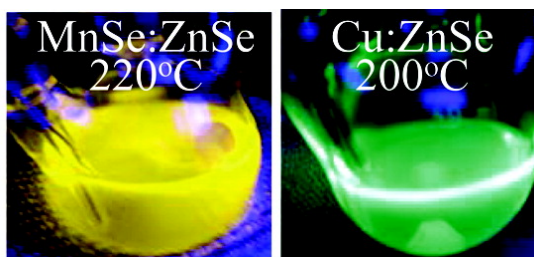
An Alternative of CdSe Nanocrystal Emitters: Pure and Tunable Impurity Emissions in ZnSe Nanocrystals

Narayan Pradhan, David Goorskey, Jason Thessing, and Xiaogang Peng

J. Am. Chem. Soc., **2005**, 127 (50), 17586-17587 • DOI: 10.1021/ja055557z • Publication Date (Web): 24 November 2005

Downloaded from <http://pubs.acs.org> on March 25, 2009

*Doped
Semiconductor
nanocrystals*



More About This Article

Additional resources and features associated with this article are available within the HTML version:

- Supporting Information
- Links to the 30 articles that cite this article, as of the time of this article download
- Access to high resolution figures
- Links to articles and content related to this article
- Copyright permission to reproduce figures and/or text from this article

[View the Full Text HTML](#)



ACS Publications
High quality. High impact.

An Alternative of CdSe Nanocrystal Emitters: Pure and Tunable Impurity Emissions in ZnSe Nanocrystals

Narayan Pradhan,[†] David Goorskey,[‡] Jason Thessing,[†] and Xiaogang Peng^{*†}

Department of Chemistry and Biochemistry, University of Arkansas, and NN-Labs, LLC, Fayetteville, Arkansas 72701

Received August 15, 2005; E-mail: xpeng@uark.edu

Semiconductor nanocrystals, with CdSe ones as the workhorse, have been widely studied for their fundamental properties¹ and applications, mostly as tunable emitters for biomedical labeling,² light emitting diodes (LEDs),^{3a} lasers,^{3b} and sensors.^{3c} Despite their apparent advantages versus organic dyes,² the intrinsic toxicity of cadmium has cast a doubtful future for this promising field. Wide band gap semiconductor nanocrystals, such as zinc chalcogenide ones, doped with transition metal ions,⁴ may overcome this concern and yet maintain the advantages of the nanocrystal emitters. However, it has been a challenge to dope all nanocrystals simultaneously, even with the vigorous organometallic approaches,^{4a,d,5} provided the extremely small volume of nanocrystals and dynamic nature in the growth process. To meet this challenge, we report methods to decouple the doping process from nucleation and/or growth, which allows us to dope nearly all nanocrystals in a given sample.

Recent success on the synthesis of high quality nanocrystals has been regarded as a result of temporal separation of nucleation and growth.⁶ This invited us to consider the possibility to decouple doping from nucleation and/or growth. Two different strategies were designed, nucleation-doping and growth-doping, respectively (Figure 1, top). These strategies were realized with the constraint of using greener precursors,⁷ such as metal carboxylate salts, and a one-pot approach. Radovanovic and Gamelin demonstrated a strategy similar to the growth doping to solve the unfavorable incorporation of Co²⁺ in CdS nanocrystals.^{8a}

For growth-doping strategy, the formation of the small host ZnSe nanocrystals occurred under established synthetic conditions^{7a} and was quenched by lowering the reaction temperature. Under the new conditions, active dopant precursors were introduced and doping occurred without the growth of the host. Using copper-doped ZnSe (Cu:ZnSe) as the model system (Figure 1 (left, middle panel), successful doping and decoupling of doping from possible nucleation and growth are indicated by several facts: the steady increase of the photoluminescence (PL) intensity from the doping centers at about 530 nm, the fixed PL positions of the host ZnSe nanocrystals and the doping centers, and the gradual decrease of the PL intensity of the host ZnSe nanocrystals. The regrowth of ZnSe on the surface of the doping layer is also shown in Figure 1 (middle right). PL of the Cu:ZnSe nanocrystals is the recombination of an excited electron in the conduction band of a ZnSe host nanocrystal and the hole from the d-orbital of a copper ion in the same nanocrystal.^{8b,c} Thus, the PL of Cu:ZnSe nanocrystals shifts to red as the size of the host increases.

Nucleation doping was realized by a mixed dopant and host precursor during the nucleation. After nucleation, the reaction conditions were tuned to be sufficiently mild to make the dopant precursors inactive, and the growth of the host became the only process, which overcoated the dopants. The concentration of the dopants in the nuclei can be tuned by varying the precursor ratio. In an extreme

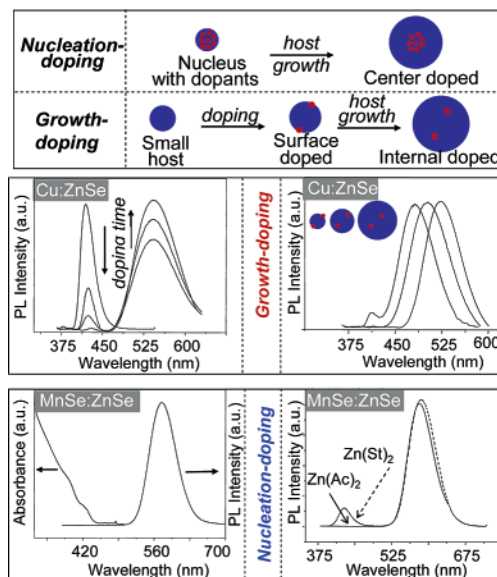


Figure 1. Schematic (top) and spectroscopic (middle and bottom) presentation of nucleation- and growth-doping. The doping time in middle left was 0, 25, 45, and 110 min, respectively.

case, the nuclei could be formed with pure dopant cations. The resulting structures can be considered as a combination of doped nanocrystals and core/shell nanocrystals. For simplicity, these nanocrystals will also be called doped nanocrystals because of their similar emission properties. The MnSe:ZnSe nanocrystals in Figure 1 (bottom panel) are an example of such core(dopant)/shell nanocrystals, whose UV-vis has the correct characteristics of a quantum-well spectrum.⁹ The PL consists of a pure dopant emission band without any evidence of host (ZnSe quantum well) nanocrystal emission.

Decoupling doping from nucleation and/or growth was realized by varying reactivity⁷ of the precursors and temperature for these one-pot approaches. The doping process for Cu:ZnSe took about 100 min to complete (Figure 1, middle), which would become uncontrollable without the decoupling technique.

For Mn:ZnSe or MnSe:ZnSe, Mn²⁺ is a harder Lewis acid compared to Zn²⁺. Therefore, the Mn²⁺ precursor should be significantly less reactive than Zn²⁺ if they both have the same carboxylate ligand. An opposite situation would be faced for Cu:ZnSe. For instance, zinc acetate (Zn(Ac)₂) was found to be a proper precursor for the formation of MnSe:ZnSe nanocrystals (Figure 1, right, bottom panel) when manganese stearate (Mn(St)₂) was used as the precursor for the nucleation stage. This allowed for a low reaction temperature (180 °C) versus the case for Zn(St)₂ (≥240 °C) for the growth of the ZnSe host shell. The higher reaction temperature needed for Zn(St)₂ caused the homogeneous nucleation of ZnSe, indicated by the band gap PL from pure ZnSe host nanocrystals (Figure 1, bottom right).

[†] University of Arkansas.

[‡] NN-Labs, LLC.

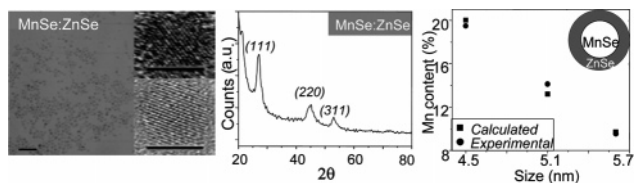


Figure 2. TEM (left), XRD (middle), and dopant concentrations (right) of MnSe:ZnSe nanocrystals. Scale bar = 50 nm (5 nm for inserts).

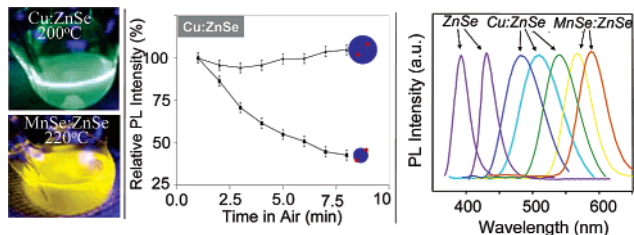


Figure 3. (Right) PL spectra of ZnSe-based emitters. (Middle) Stability of Cu:ZnSe in air. (Left) PL from doped nanocrystals at above 200 °C.

The lattice fringes of the doped nanocrystals in the transmission electron microscope (TEM) images run across the entire crystals with no significant contrast variation (Figure 2, left (insets)). The X-ray powder diffraction (XRD) (Figure 2, middle) and electron diffraction patterns all confirmed the crystals had a zinc blend structure similar to ZnSe. Interestingly, the lattice constants of zinc blend ZnSe and MnSe are almost identical. The pure MnSe core of MnSe:ZnSe nanocrystals varied from about 1 to 4 nm without affecting the PL brightness and structure. This feature and the quantum well type of absorption spectrum indicate that these unique structures may significantly differ from traditional doped nanocrystals, although their PL properties are similar. The Mn content matched well with the calculations by assuming uniform growth of pure ZnSe shell around a given sized MnSe core (Figure 2, right).

The PL quantum yield of the doped nanocrystals was found to be between 10% and 30% although the conditions were not necessarily ideal for optimal PL brightness. The PL peak position of Cu:ZnSe nanocrystals can be readily tuned between about 470 and 550 nm (Figures 1 and 3) because of the expected quantum confinement discussed above. It was surprising to observe that the strong PL from MnSe:ZnSe nanocrystals could also be tuned, from about 575 nm to 595 nm (Figure 3). A possible explanation is that as the ZnSe outer-shell grew thicker, the crystal field for each dopant ion became more symmetric in long range. Consequently, the crystal field splitting of the d-orbitals became smaller, which resulted in a PL red shift.

The PL of surface-doped nanocrystals was a few times weaker than that of the corresponding internal- and center-doped nanocrystals. The location of the dopants also strongly affected their PL responses to the environment. The reasonably strong PL from the surface-doped Cu:ZnSe nanocrystals was quenched almost completely by exposure to air within several minutes to a few hours (Figure 3, middle), while the same treatment did not affect the PL of the corresponding internal-doped Cu:ZnSe nanocrystals with the ZnSe shell on the surface. Similar results were observed when treating the nanocrystals with pyridine, thiol, and UV-radiation. Under all conditions tested, the PL of the center-doped and internal-doped nanocrystals were stable and the surface-doped ones were very fragile (see Supporting Information).

Thermal treatments of doped nanocrystals up to 200 °C for a few hours did not substantially change the PL properties of the doped nanocrystals (Figure 3), although a very strong thermal quenching was observed for plain CdSe or ZnSe nanocrystals (Supporting Information). As pointed out above, the PL position

of high quality doped nanocrystals likely depends on where the dopants are. Therefore, their thermal stability supports that the mobility of the dopants in the lattice was low within the experimental temperature range. A possible reason for the exceptional thermal and environmental stability of the PL of the center-doped and internal-doped nanocrystals may be due to their d–d transition nature, which does not strongly couple with the phonons and surfaces, unlike a regular exciton emission.

Thermal and environmental stability brings in noticeable advantages for nearly all applications using nanocrystal emitters. The doped nanocrystal emitters will be dramatically more durable upon their unavoidable thermal effects of LEDs and lasers. Environmental effects on PL of quantum dots have been a major barrier for their biomedical applications. Reabsorption and Forster energy transfer should not exist between doped ZnSe nanocrystals because of their dramatic Stokes's shift (Figure 1, bottom left). This feature makes the doped nanocrystals ideal candidates for lasing,^{3b} bar-coding,¹⁰ and other applications where high concentrations of nanocrystals are needed.

In summary, results illustrate that decoupling doping from nucleation and/or growth can be achieved. The color-tunable ZnSe based emitters covers most of the visible window (Figure 3). The resulting nanocrystals are one step further for green synthetic chemistry for semiconductor nanocrystals,^{7b} from greener methods to greener products. These alternative emitters are not only less toxic than CdSe based ones, but also much less sensitive to thermal and environmental variations and do not render Forster energy transfer and reabsorption. In addition to the potential applications as emitters, these new nanostructures imply possibilities to build up complex functions into a nanocrystal. For instance, the MnSe:ZnSe nanocrystals may be of interest for spintronics.¹¹ Cu:ZnSe may provide unique opportunities to independently study quantum confinement of the conduction and the valence band of nanocrystals.

Supporting Information Available: This work was partially supported by the NSF. HRTEM was taken by K. Jones. Experimental, thermal, and chemical stability, and more supporting results. This material is available free of charge via the Internet at <http://pubs.acs.org>.

References

- (1) (a) Brus, L. E. *J. Chem. Phys.* **1983**, *79*, 5566–5571. (b) Alivisatos, A. P. *Science* **1996**, *271*, 933–937. (c) Murray, C. B.; Norris, D. J.; Bawendi, M. G. *J. Am. Chem. Soc.* **1993**, *115*, 8706–8715.
- (2) (a) Bruchez, M., Jr.; Moronne, M.; Gin, P.; Weiss, S.; Alivisatos, A. P. *Science* **1998**, *281*, 2013–2016. (b) Chan, W. C. W.; Nile, S. *Science* **1998**, *281*, 2016–2018.
- (3) (a) Colvin, V. L.; Schlamp, M. C.; Alivisatos, A. P. *Nature* **1994**, *370*, 354–357. (b) Klimov, V. I.; Mikhailovsky, A. A.; Xu, S.; Malko, A.; Hollingsworth, J. A.; Leatherdale, C. A.; Eisler, H. J.; Bawendi, M. G. *Science* **2000**, *290*, 314–317. (c) Nazzari, A. Y.; Qu, L.; Peng, X.; Xiao, M. *Nano Lett.* **2003**, *3*, 819–822.
- (4) (a) Erwin, S. C.; Zu, L.; Haftel, M. I.; Efros, A. L.; Kennedy, T. A.; Norris, D. J. *Nature* **2005**, *436*, 91–94. (b) Schwartz, D. A.; Norberg, N. S.; Nguyen, Q. P.; Parker, J. M.; Gamelin, D. R. *J. Am. Chem. Soc.* **2003**, *125*, 13205–13218. (c) Bhargava, R. N.; Gallagher, D.; Hong, X.; Nurmikko, A. *Phys. Rev. Lett.* **1994**, *72*, 416–419. (d) Norris, D. J.; Yao, N.; Charnock, F. T.; Kennedy, T. A. *Nano Lett.* **2001**, *1*, 3–7. (e) Holtz, P. O.; Monemar, B.; Loykowski, H. *J. Phys. Rev. B* **1985**, *32*, 986–996. (f) Hefetz, Y.; Nakahara, J.; Nurmikko, A. V.; Kolodziejewski, L. A.; Gunshor, R. L.; Datta, S. *Appl. Phys. Lett.* **1985**, *47*, 989–991. (g) Bol, A. A.; Meijerink, A. *J. Phys. Chem. B* **2001**, *105*, 10197–10202.
- (5) Mikulec, F. V.; Kuno, M.; Bennati, M.; Hall, D. A.; Griffin, R. G.; Bawendi, M. G. *J. Am. Chem. Soc.* **2000**, *122*, 2532–2540.
- (6) Peng, X.; Wickham, J.; Alivisatos, A. P. *J. Am. Chem. Soc.* **1998**, *120*, 5343–5344.
- (7) (a) Li, L.; Pradhan, N.; Wang, Y.; Peng, X. *Nano Lett.* **2004**, *4*, 2261–2264. (b) Peng, X. *Eur. J. Chem. Soc.* **2002**, *8*, 334–339.
- (8) (a) Radovanovic, P. V.; Gamelin, D. R. *J. Am. Chem. Soc.* **2001**, *123*, 12207–12214. (b) Stringfellow, G. B.; Bube, R. H. *Phys. Rev.* **1968**, *171*, 903–915. (c) Suyver, J. F.; Beek, T. V.; Wuijster, S. F.; Kelly, J. J.; Meijerink, A. *Appl. Phys. Lett.* **2001**, *79*, 4222–4224.
- (9) Battaglia, D.; Li, J. J.; Wang, Y.; Peng, X. *Angew. Chem., Int. Ed.* **2003**, *42*, 5035–5039.
- (10) Han, M.; Gao, X.; Su, J. Z.; Nie, S. *Nat. Biotechnol.* **2001**, *19*, 631–635.
- (11) Sato, K.; Yoshida, H. K. *Semicond. Sci. Technol.* **2002**, *17*, 367–376.

JA05557Z